34th Annual International Conference of the IEEE EMBS
San Diego, California USA, 28 August - 1 September, 2012

Single Molecule Tracking of P-glycoprotein in Live Cells Reveals Dynamic Heterogeneity

Philip P. Cheney, Michael D. Stachler, and Michelle K. Knowles, *Member, IEEE*

Abstract— **P-glycoprotein transports chemotherapy drugs from the plasma membrane and allows cancer cells to survive treatment. We transiently transfected PGP labeled with enhanced green fluorescent protein (PGP-EGFP) into MES-SA cells and used single molecule tracking techniques to characterize the dynamics on the surface of live cells. PGP exhibits freely diffusive behavior at short times and is confined at long times with a transition to anomalous diffusion at 0.7 s.**

I. INTRODUCTION

In response to chemotherapy, tumor cells often up-regulate multidrug resistance transporters to survive treatment. P-glycoprotein (PGP) is an ATP dependent, drug transporter present in many forms of untreatable cancer [1, 2]. PGP contains 12 transmembrane domains and is a large (170 kDa) protein that binds lipophilic drug molecules from the plasma membrane to export them from the cell, effectively reducing the intracellular concentration of drug [1]. The presence of PGP can be predictive of the outcome of chemotherapy treatment, with increased amounts correlating to poor prognosis. [3-5].

PGP interacts with many proteins and lipids on the cell surface, including the actin cytoskeleton and lipid rafts [6, 7]. PGP has been shown to be enriched in lipid rafts and intermediate-density rafts [7-10]. Specifically, cholesterol has been shown to modulate the membrane transport activity of PGP, increasing the efflux activity six-fold in a reconstituted membrane system [11, 12]. In a model cellular system transiently expressing PGP, the loss of cholesterol abolishes PGP efflux activity [13]. Others have reported that the presence of cholesterol affects both the ability of chemotherapy drugs to bind to PGP and transport rate of PGP [8].Research suggests that the efflux activity of PGP is highly sensitive to the local environment [13, 14]. When multidrug resistant leukemia cells are treated with an antibody to CD19, a protein that interacts with PGP, PGP translocates from lipid rafts and its activity is halted, allowing the cells to become chemosensitive [14]. The local environment clearly affects PGP activity.

In addition to known PGP interactions, the heterogeneous structure of the plasma membrane likely contributes to the anomalous diffusion of membrane proteins. The cytoskeleton has been shown to create corrals and lipid rafts can be related to transient confinement zones [15, 16]. Single molecule tracking allows for a direct visualization of these phenomena in regards to membrane proteins moving on the plasma membrane.

To better understand the transient interactions of PGP on the cell surface, the dynamics of PGP were assessed using single particle tracking (SPT) techniques. Single molecule tracking of drug transporters in the plasma membrane of live cells allows for the direct measurement of transient and heterogeneous interactions that have the potential for altering the efficiency of drug transport. Techniques that measure the heterogeneity of the system will lead to a better understanding of PGP interactions on the cell surface. In this work, we describe an assay for measuring the dynamics of single PGP molecules using SPT techniques in a model cell system, MES-SA cells. We show here that PGP-EGFP can be imaged and tracked in live cells to better understand PGP interactions on the plasma membrane. We find that when PGP-EGFP is expressed on the cell surface, rhodamine, a substrate, is effectively removed from the cell, showing that PGP-EGFP is functional in MES-SA cells. Using SPT, PGP is observed to be quite mobile for a large transmembrane protein but exhibits confined diffusion over long time periods (> 0.7 s). At short times, PGP moves freely with a diffusion coefficient, D, of 0.2 $\mu m^2/s$. To our knowledge, this is the first report of single molecule of PGP dynamics.

II. METHODS

A. Cell Culture and Transfection

The adherent MES-SA cell line (ATCC) was used for all tracking experiments. Cells were maintained at 37 °C in a humidified atmosphere containing 5% CO_2 in McCoy's 5A medium containing 1.5 mM L-glutamine, 100U/mL penicillin, 100 µg/mL streptomycin, and 10% fetal bovine serum. Cells were plated on poly-L-lysine (Sigma Aldrich)

*Research supported by start-up funds from the University of Denver, a fellowship from the Chickasaw Nation for Philip P. Cheney.

Philip P. Cheney is with the Department of Chemistry and Biochemistry, University of Denver, Denver, CO 80208 USA (e-mail: Philip.Cheney@du.edu).

Michael D. Stachler is with the Department of Chemistry and Biochemistry, University of Denver, Denver, CO 80208 USA (e-mail: Michael.Stachler@du.edu).

Michelle K. Knowles is with the Department of Chemistry and Biochemistry, University of Denver, Denver, CO 80208 USA (e-mail: Michelle.Knowles@du.edu).

coated coverslips. Transfection with PGP-EGFP was carried out on coverslip-plated MES-SA cells using Lipofectamine 2000 (Invitrogen, Carlsbad, CA) and 1.5 µg of DNA plasmid per coverslip in serum-free OptiMEM. The plasmid was obtained from Dr. Michael Gottesman [17]. Cells were incubated in the transfection solution for six hours at 37 °C and imaged between 24 and 48 hours post-transfection. All cell culture reagents were purchased from Invitrogen.

B. Total Internal Reflection Fluorescence Microscopy (TIRFM)

Cells expressing PGP-EGFP were imaged using objective-style TIRFM. TIRFM allows only 100-200 nm of the cell in contact with the glass coverslip to be excited. A Nikon Eclipse Ti-U microscope equipped with a TIRF launch, a 60x oil immersion TIRFM objective (NA 1.49), and 2.5x magnification lens was used for a final magnification of 150x. A 491 nm laser (Cobolt Calypso DPSS) provided excitation of EGFP. Fluorescence emission was captured through a dichroic that passes 500-545 nm made specifically for TIRFM application (Chroma Technologies). Afterwards, fluorescence emission passed through a 525/50 nm filter (Chroma Technologies) onto a back-illuminated EMCCD camera (Andor iXon+ 897). Imaging was performed at 25 °C. Image series were captured as a stream of 100 ms exposures using µManager (http://www.micro-manager.org). Movies were 500 frames in length. A typical image that was used for single particle tracking is shown in Fig. 1.

C. Single Particle Tracking

The series of images captured using TIRFM was analyzed in ImageJ (http://imagej.nih.gov/ij/) using the particle tracking plug-in from MOSAIC [18]. Particle detection parameters were as follows: the kernel radius was 3.0 pixels, the cutoff radius was 0.0 pixels, and the top one percentile of bright pixels was considered as particle candidates. Tracked particles were allowed to travel a maximum of six pixels (0.642 µm) between consecutive frames to be considered as linked particles.

The position matrices representing particle tracks produced in ImageJ were then transferred into IDL (Exelis) in order to use freely available software to analyze tracks (http://www.physics.emory.edu/~weeks/idl/tracking.html) as has been done previously by others to track membrane protein dynamics [19, 20]. The displacement of each particle at varying time lags, t, were calculated. Mean square displacements (MSD) was calculated as described [21].

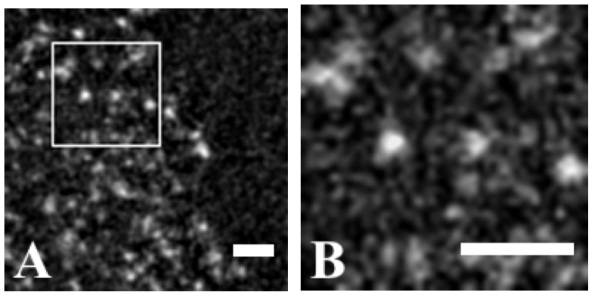

Figure 1. PGP-EGFP particles are imaged on the plasma membrane of a cell (A). The enlarged region (B) shows individual particles with more detail. The scale bar on both images represents 2 µm.

Displacement histograms and MSD values were plotted and fit in Prism 5 (GraphPad Software, La Jolla, California USA). Displacement histograms were fit to (1) to determine the diffusion coefficients, D_1 and D_2, as well as the amplitude of fast and slow molecules in the population, A_1 and A_2 as previously described [19, 22].

$$y(r,t) = r\left[A_1\, exp\left(-\frac{r^2}{4D_1 t}\right) + A_2\, exp\left(-\frac{r^2}{4D_2 t}\right)\right] \quad (1)$$

Mean square displacements (2) were fit with a segmental linear regression to distinguish the two diffusing populations of PGP. The segmental linear regression was carried out as provided in Prism 5 and was allowed to find the transition between the two linear sections by the least squares method.

$$\langle r^2 \rangle = 4Dt \quad (2)$$

D. Rhodamine Efflux Studies

Efflux activity of PGP-EGFP was tested in MES-SA cells as previously described [22]. Transfected cells expressing PGP-EGFP were incubated in a 1 µM solution of rhodamine 6G (R6G) in phosphate buffered saline (PBS) for five minutes prior to confocal imaging. The R6G solution was left on the cells during imaging and confocal images of the cells were taken using both the EGFP and R6G fluorescent emission channels. Untransfected MES-SA cells were imaged in the same manner as negative efflux controls.

E. Confocal Imaging

Confocal imaging of R6G efflux was performed on an Olympus FluoView FV1000 confocal microscope using a 100x oil immersion objective (NA 1.40). Excitation was at 488 nm and 515 nm and fluorescence emission was collected from 495 nm to 510 nm and from 530 nm to 560 nm. The surface of live cells nearest the coverslip were imaged at 25 °C.

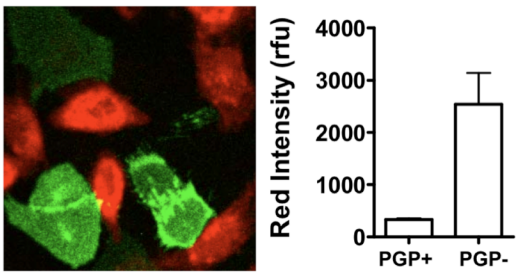

Figure 2. PGP actively removes rhodamine 6G (R6G) from cells. Cells expressing PGP-EFGP (green) display low levels of R6G uptake, even after 30 min in 1 µM R6G. Quantitation shows that significantly more R6G (red) accumulates in cells not expressing PGP-EGFP. Error is shown as the SEM.

III. Results

A. PGP-EGFP removes rhodamine from the plasma membrane of live MES-SA cells.

In cells transfected with PGP-EGFP, R6G is effectively excluded from the plasma membrane. As shown in Fig. 2, cells that are expressing PGP-EGFP have very little R6G fluorescence. Cells that are not expressing PGP-EGFP, identified by the absence of EGFP fluorescence, have significantly more R6G fluorescence. This shows that PGP-EGFP is functional in MES-SA cells.

B. PGP-EGFP is mobile at short times and confined at long times (>0.7 s)

Over short periods of time, it appears that PGP-EGFP on the surface of cells diffuses at a rate faster than when observed over longer period of times. Fig. 3 suggests that there is a transition between these rates at approximately 0.7 s. The displacement histograms in Fig. 4 show what appear to be two diverging populations of diffusing particles, one slowly diffusing population and another that is diffusing even more slowly. This suggests PGP-EGFP molecules are fully or partially confined as seen in Fig. 5. The dashed lines in Fig. 4 show how a population of particles diffusing at 0.2 $\mu m^2/s$ would be distributed at various time points. The growing difference between these two curves further suggests a population of slowly moving or confined particles.

IV. Discussion

Functional PGP-EGFP can be transiently expressed in cells that are devoid of PGP (MES-SA). PGP-EGFP effectively removes R6G from the cell membrane and cells that do not express PGP retain the red fluorescent rhodamine, as shown in Fig. 2 using transient transfection techniques. Cells express a diverse amount of PGP-EGFP, which allows us to study PGP-EGFP on a single molecule level amenable to particle tracking. Cells with low levels of PGP are imaged and molecules are tracked to reveal heterogeneous behavior; the heterogeneity is most obvious near the transition time from freely diffusing to confined motion (0.7 s). PGP freely diffuses on short time and length scales but is confined at longer times, as seen in the MSD in Fig. 4. When the step size of a molecule is measured at a very short time lag, most molecules are freely diffusing. However, when the distance traveled over a long time lag is measured, most are confined. The heterogeneity of the system lies in the intermediate time scales. The histograms in Fig. 4 reveal a confined motion not observed in MSD at long times.

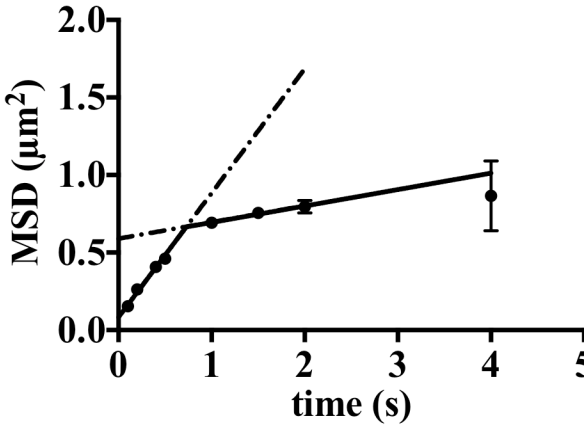

Figure 3. Two distinct populations of diffusion are present. A segmented linear regression shows a transition from fast diffusion to slow, or confined, diffusion at 0.7 s. Error is shown as the SEM.

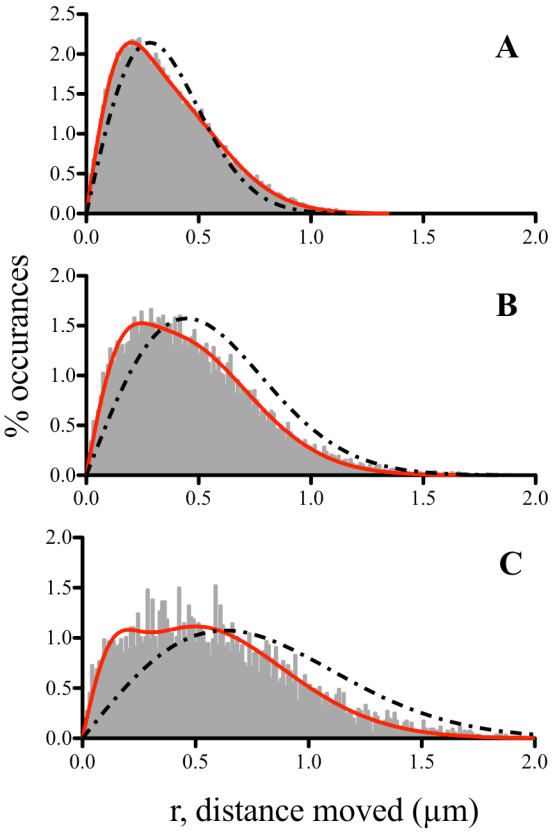

Figure 4. The displacement of particles is measured for various time intervals, revealing diverging populations of diffusing particles. Displacement histograms are fit to (1) (solid red line) for 0.2 s (A), 0.5 s (B), and 1.0 s (C). A simulated curve of (1) with a single population diffusing at 0.2 $\mu m^2/s$ is provided (dashed black line) for reference.

Future investigations using two-color single particle tracking techniques could reveal what PGP is interacting with. Interactions with the actin cytoskeleton and lipid microdomains are likely influencing the dynamics of PGP and could be a factor in how readily PGP transports chemotherapy drugs.

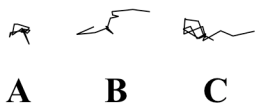

Figure 5. Two-dimensional trajectories of particles can show confinement (A), free diffusion (B), or a combination of these two (C). Note in C a particle diffuses freely for several steps then becomes confined.

V. Conclusion

The dynamics of PGP suggest that diverse interactions are occurring on the surface of cells and single particle tracking allows for the direct observation of such interactions. Further investigations on the effects of drugs that activate or inhibit PGP could lead to a better understanding of how this complex membrane protein can be regulated to reduce the impact of multi-drug resistance in cancer treatment.

References

[1] M. M. Gottesman, T. Fojo, and S. E. Bates, "Multidrug resistance in cancer: role of ATP-dependent transporters," *Nat Rev Cancer,* vol. 2, pp. 48-58, Jan 2002.

[2] M. K. Al-Shawi and H. Omote, "The remarkable transport mechanism of P-glycoprotein: a multidrug transporter," *J Bioenerg Biomembr,* vol. 37, pp. 489-96, Dec 2005.

[3] S. V. Ambudkar, S. Dey, C. A. Hrycyna, M. Ramachandra, I. Pastan, and M. M. Gottesman, "Biochemical, cellular, and pharmacological aspects of the multidrug transporter," *Annu Rev Pharmacol Toxicol,* vol. 39, pp. 361-98, 1999.

[4] H. S. Chan, G. Haddad, P. S. Thorner, G. DeBoer, Y. P. Lin, N. Ondrusek, H. Yeger, and V. Ling, "P-glycoprotein expression as a predictor of the outcome of therapy for neuroblastoma," *N Engl J Med,* vol. 325, pp. 1608-14, Dec 5 1991.

[5] T. Fojo and H. M. Coley, "The role of efflux pumps in drug-resistant metastatic breast cancer: new insights and treatment strategies," *Clin Breast Cancer,* vol. 7, pp. 749-56, Oct 2007.

[6] F. Luciani, A. Molinari, F. Lozupone, A. Calcabrini, L. Lugini, A. Stringaro, P. Puddu, G. Arancia, M. Cianfriglia, and S. Fais, "P-glycoprotein-actin association through ERM family proteins: a role in P-glycoprotein function in human cells of lymphoid origin," *Blood,* vol. 99, pp. 641-8, Jan 15 2002.

[7] Z. Bacso, H. Nagy, K. Goda, L. Bene, F. Fenyvesi, J. Matko, and G. Szabo, "Raft and cytoskeleton associations of an ABC transporter: P-glycoprotein," *Cytometry A,* vol. 61, pp. 105-16, Oct 2004.

[8] P. D. Eckford and F. J. Sharom, "Interaction of the P-glycoprotein multidrug efflux pump with cholesterol: effects on ATPase activity, drug binding and transport," *Biochemistry,* vol. 47, pp. 13686-98, Dec 23 2008.

[9] F. Fenyvesi, E. Fenyvesi, L. Szente, K. Goda, Z. Bacso, I. Bacskay, J. Varadi, T. Kiss, E. Molnar, T. Janaky, G. Szabo, Jr., and M. Vecsernyes, "P-glycoprotein inhibition by membrane cholesterol modulation," *Eur J Pharm Sci,* vol. 34, pp. 236-42, Aug 7 2008.

[10] G. Radeva, J. Perabo, and F. J. Sharom, "P-Glycoprotein is localized in intermediate-density membrane microdomains distinct from classical lipid rafts and caveolar domains," *FEBS J,* vol. 272, pp. 4924-37, Oct 2005.

[11] K. Bucher, S. Belli, H. Wunderli-Allenspach, and S. D. Kramer, "P-glycoprotein in proteoliposomes with low residual detergent: the effects of cholesterol," *Pharm Res,* vol. 24, pp. 1993-2004, Nov 2007.

[12] J. Troost, N. Albermann, W. Emil Haefeli, and J. Weiss, "Cholesterol modulates P-glycoprotein activity in human peripheral blood mononuclear cells," *Biochem Biophys Res Commun,* vol. 316, pp. 705-11, Apr 9 2004.

[13] M. A. Ghetie, R. Marches, S. Kufert, and E. S. Vitetta, "An anti-CD19 antibody inhibits the interaction between P-glycoprotein (P-gp) and CD19, causes P-gp to translocate out of lipid rafts, and chemosensitizes a multidrug-resistant (MDR) lymphoma cell line," *Blood,* vol. 104, pp. 178-83, Jul 1 2004.

[14] S. W. Kamau, S. D. Kramer, M. Gunthert, and H. Wunderli-Allenspach, "Effect of the modulation of the membrane lipid composition on the localization and function of P-glycoprotein in MDR1-MDCK cells," *In Vitro Cell Dev Biol Anim,* vol. 41, pp. 207-16, Jul-Aug 2005.

[15] C. Dietrich, B. Yang, T. Fujiwara, A. Kusumi, and K. Jacobson, "Relationship of lipid rafts to transient confinement zones detected by single particle tracking," *Biophys J,* vol. 82, pp. 274-84, Jan 2002.

[16] M. M. Tamkun, M. O'Connell K, and A. S. Rolig, "A cytoskeletal-based perimeter fence selectively corrals a sub-population of cell surface Kv2.1 channels," *J Cell Sci,* vol. 120, pp. 2413-23, Jul 15 2007.

[17] J. Petriz, M. M. Gottesman, and J. M. Aran, "An MDR-EGFP gene fusion allows for direct cellular localization, function and stability assessment of P-glycoprotein," *Curr Drug Deliv,* vol. 1, pp. 43-56, Jan 2004.

[18] I. F. Sbalzarini and P. Koumoutsakos, "Feature point tracking and trajectory analysis for video imaging in cell biology," *J Struct Biol,* vol. 151, pp. 182-95, Aug 2005.

[19] M. K. Knowles, S. Barg, L. Wan, M. Midorikawa, X. Chen, and W. Almers, "Single secretory granules of live cells recruit syntaxin-1 and synaptosomal associated protein 25 (SNAP-25) in large copy numbers," *Proc Natl Acad Sci U S A,* vol. 107, pp. 20810-5, Nov 30 2010.

[20] A. D. Douglass and R. D. Vale, "Single-molecule microscopy reveals plasma membrane microdomains created by protein-protein networks that exclude or trap signaling molecules in T cells," *Cell,* vol. 121, pp. 937-50, Jun 17 2005.

[21] J. C. Crocker and D. G. Grier, "Methods of Digital Video Microscopy for Colloidal Studies," *J. Colloid Interface Sci.,* vol. 179, p. 298, 1996.

[22] C. Ludescher, Gattringer, J. Drach, J. Hofmann, and H. Grunicke, "Rapid functional assay for the detection of multidrug-resistant cells using the fluorescent dye rhodamine 123," *Blood,* vol. 78, pp. 1385-7, Sep 1 1991.